Magnetoelectric coupling in MnTiO₃

N. Mufti,[1,*] G. R. Blake,[1] M. Mostovoy,[1] S. Riyadi,[1] A. A. Nugroho,[2] and T. T. M. Palstra[1]

[1]*Zernike Institute for Advanced Materials, Rijksuniversiteit Groningen, Nijenborgh 4, NL-9747AG Groningen, The Netherlands*

[2]*Faculty of Mathematics and Natural Sciences, Institut Teknologi Bandung, Jl. Ganesha 10, Bandung 40132, Indonesia*

We give general arguments that show that the linear magnetoelectric effect in antiferromagnetic materials gives rise to a magnetocapacitance anomaly—a divergence of the dielectric constant at the magnetic ordering temperature T_N that appears in an applied magnetic field. The measurement of magnetodielectric response thus provides a definitive and experimentally accessible method to recognize antiferromagnetic linear magnetoelectric materials, circumventing the experimental difficulties often involved in measuring electric polarization. We confirm this result experimentally using the example of MnTiO₃, which we show to exhibit the linear magnetoelectric effect. No dielectric anomaly is observed at T_N in the absence of an applied magnetic field. However, a sharp peak in the dielectric constant appears here when a magnetic field is applied along the c axis, reflecting a linear coupling of the polarization P with the antiferromagnetic order parameter L. In accordance with our theoretical analysis, the dielectric constant close to T_N increases with the square of the magnetic field.

I. INTRODUCTION

Recent years have seen a resurgence of interest in the study of multiferroic materials, in part due to the discovery of the strong interplay between magnetism and ferroelectricity in the so-called type-II multiferroics where electrical polarization is induced by magnetic ordering.[1] A common characteristic of these materials is the presence of competing magnetic exchange interactions of similar magnitude which give rise to unconventional spin states breaking inversion symmetry.[2–9] Such states are highly susceptible to applied magnetic fields, which often makes it possible to rotate or reverse the induced electrical polarization.[10–14]

In some multiferroics the rotation of polarization is accompanied by a dramatic enhancement of the dielectric constant ε. For example, this so-called giant magnetocapacitance effect was observed in perovskite DyMnO₃,[15] where Mn spins form a spiral parallel to the bc plane, inducing electrical polarization P along the c axis. In an applied magnetic field $H\|b$ this material exhibits a flop transition into the ab-spiral state with $P\|a$.[10] At the critical magnetic field the direction of the polarization vector can be controlled by an applied electric field favoring one of the two spiral states, which is what makes ε large. The magnetocapacitance $\frac{\varepsilon(H)-\varepsilon(0)}{\varepsilon(0)}$ reaches its highest value of ∼500% near the critical point where the two ferroelectric spiral states and the paraelectric state with collinear spins merge to give rise to large spin fluctuations. Recent measurements of the frequency dependence of the dielectric constant anomaly indicate that the giant magnetocapacitance effect originates from the dynamics of the 90° domain walls separating the ab- and bc-spiral states, which close to the critical point can be set in motion by relatively low electric fields.[16] Large magnetocapacitance has also been observed in the incommensurate phase of DyMn₂O₅.[17]

In this paper we focus on materials that allow a different form of magnetic control of the electric polarization—the linear magnetoelectric effect. Similar to magnetically induced ferroelectricity, this effect occurs in antiferromagnets with broken inversion symmetry. Here, however, the electric polarization is zero unless an external magnetic field is applied. In the presence of magnetic field, P increases proportional to H, and *vice versa*, the magnetization M increases linearly with an applied electric field E. Both effects originate from the LEH terms in the free energy, where L is the antiferromagnetic order parameter.[18–20]

Here we show that the linear coupling between electric and magnetic fields in antiferromagnets gives rise to a *nonlinear* magnetoelectric response dominated by critical spin fluctuations. In particular, it results in the *divergence* of the magnetocapacitance at the Néel transition temperature T_N. The anomalous part of the field-dependent dielectric constant is proportional to $H^2|T - T_N|^{-\gamma}$, where γ is the critical exponent describing the transition. This characteristic divergence can be used to identify linear magnetoelectric materials, thus circumventing the experimental difficulties involved in measuring electric polarization when the latter is too small or when the resistivity is too large.

These issues prompted us to investigate MnTiO₃, a potential linear magnetoelectric material. MnTiO₃ adopts the ilmenite structure (space group $R\bar{3}$) in which Mn²⁺ and Ti⁴⁺ layers alternate along the c axis of the hexagonal lattice.[21–23] The Mn²⁺ spins align in antiferromagnetic fashion both along the c direction and within each layer. MnTiO₃ single crystals show a change in slope of the magnetic susceptibility at $T_N = 64$ K for fields applied parallel to the c axis and a broad minimum near 50 K for fields applied perpendicular to the c axis. This anisotropy does not disappear at T_N but persists up to 95 K, where two-dimensional order most likely sets in. Furthermore, a flop in the magnetization has been observed at $H \sim 6$ T for magnetic fields applied parallel to the c axis.[24] The magnetic symmetry below T_N is reported to be $R\bar{3}'$ (Ref. 21), which allows the linear magnetoelectric effect, with the nonzero tensor elements $\alpha_{xx} = \alpha_{yy}$, α_{zz}, and $\alpha_{xy} = -\alpha_{yx}$. Here, we demonstrate by measuring P as a function of H that MnTiO₃ is indeed a linear magnetoelectric. No dielectric anomaly is present at T_N unless an external magnetic field is applied. We then observe an anomalous enhancement in the dielectric constant near T_N that scales with H^2. We note that the dielectric behavior of MnTiO₃ is different to that of all other Mn²⁺

systems reported to exhibit dielectric anomalies at T_N. For example, BaMnF$_4$ is a multiferroic material that exhibits a divergence of the dielectric constant in zero field at T_N; the linear magnetoelectric effect is allowed by symmetry but has not yet been demonstrated experimentally.[25,26] MnO (Ref. [27]) and MnF$_2$ (Ref. [28]) are both magnetodielectric materials in which the zero-field dielectric constant changes slope at T_N due to an exchange-striction mechanism. In MnTiO$_3$, the absence of any dielectric anomaly in zero field implies that the effect of exchange striction on the dielectric properties is negligible. MnTiO$_3$ thus allows the nonlinear magnetoelectric response at T_N to be studied in isolation, allowing us to prove that the field dependence of the magnetocapacitance anomaly provides a ready experimental method by which linear magnetoelectrics can be recognized.

The rest of the paper is organized as follows. In Secs. II and III we describe the experimental setup and the results of measurements of the magnetic, dielectric, and magnetoelectric response of MnTiO$_3$. In Sec. IV we present general theoretical arguments relating the observed magnetocapacitance anomaly to the linear magnetoelectric effect. Finally, in Secs. V and VI we discuss our experimental and theoretical results and conclude.

II. EXPERIMENT

A single crystal of MnTiO$_3$ was grown by the floating zone technique. The feed rod was prepared by a standard solid state reaction of stoichiometric quantities of MnCO$_3$ and TiO$_2$ in air. The crystal growth rate was between 1.5 and 5 mm/h and was carried out in air. The seed and feed rods were counterrotated at a speed of 15–20 rpm. The resulting crystals were oriented using Laue diffraction. The dielectric constant was measured using an Andeen-Hagerling AH-2500A capacitance bridge operating at a fixed frequency of 1 kHz. The pyroelectric current was measured on warming, using a Keithley 6517A electrometer, after poling the crystal in an electric field of $\sim$250 V/mm while cooling from above T_N. The spontaneous polarization was obtained by integration of the pyroelectric current with respect to temperature. The temperature and magnetic field were controlled through a physical properties measurement system (Quantum Design), using a homemade insert and wiring.

III. EXPERIMENTAL RESULTS

The crystal structure of MnTiO$_3$ can be envisaged in either a rhombohedral or hexagonal setting; previous studies have mostly used the latter. Figure 1 shows an x-ray powder diffraction pattern of a crushed single crystal sample. All peaks could be well fitted using the model of Ko and Prewitt[29] with the $R\bar{3}$ space group; the lattice parameters of $a = 5.1396$ Å and $c = 14.2841$ Å are in good agreement with previous reports.[24,29] No impurity phase was observed from the x-ray diffraction pattern.

The temperature dependence of the magnetic susceptibility of MnTiO$_3$ parallel ($\chi\|c$) and perpendicular ($\chi\perp c$) to the hexagonal c axis is shown in Fig. 2. The value of $\chi\|c$ initially increases with temperature and shows a change of slope at
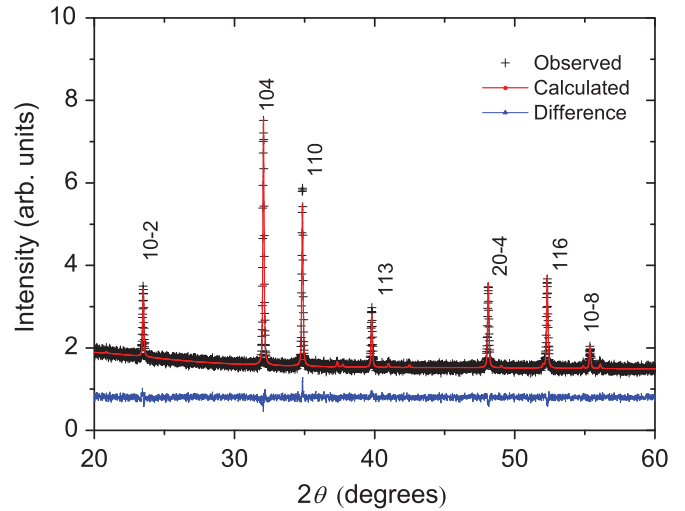

FIG. 1. (Color online) Observed, calculated, and difference x-ray powder diffraction profiles of crushed MnTiO$_3$ single crystal at room temperature.

$T_N \sim 64$ K. In contrast, $\chi\perp c$ is almost constant below T_N, then increases slightly to a broad maximum centered at $\sim$90 K.

The dielectric constant of MnTiO$_3$ was measured as a function of temperature for orientations parallel ($\varepsilon\|c$) and perpendicular ($\varepsilon\perp c$) to the hexagonal c axis (Fig. 3). No anomalies were observed at T_N for either direction. However, when a magnetic field was applied, we observed a sharp peak at T_N for $H, E\|c$ [Fig. 3(b)]. This peak increases in intensity with magnetic field up to 6 T before decreasing again at higher fields. For $E, H\perp c$, no anomaly was observed up to 5 T [Fig. 3(a)]. We also measured the dielectric constant for $H\perp c$, $E\|c$ and for $H\|c$, $E\perp c$ (not shown in this paper) and no anomalies were observed in either case. We note that for each measurement we cooled the samples from the paramagnetic state at $T \sim 100$ K while continuously applying the magnetic field to obtain a single magnetic domain.

To prove the presence of the linear magnetoelectric effect in MnTiO$_3$, it is necessary to measure the electrical polarization. Figure 4 shows the temperature dependence of the pyroelectric
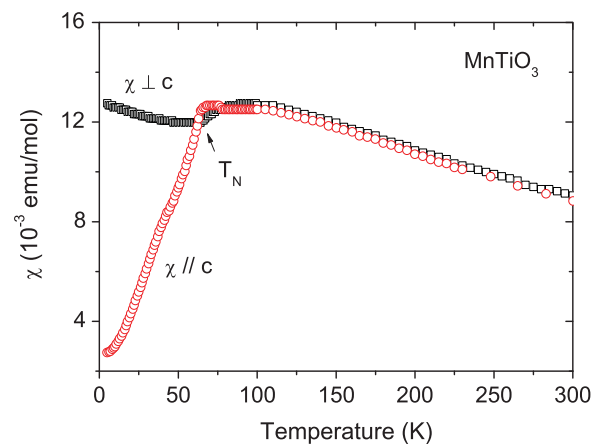

FIG. 2. (Color online) Temperature dependence of parallel and perpendicular magnetic susceptibilities of MnTiO$_3$. The measurements were performed in an applied field of 0.1 T.
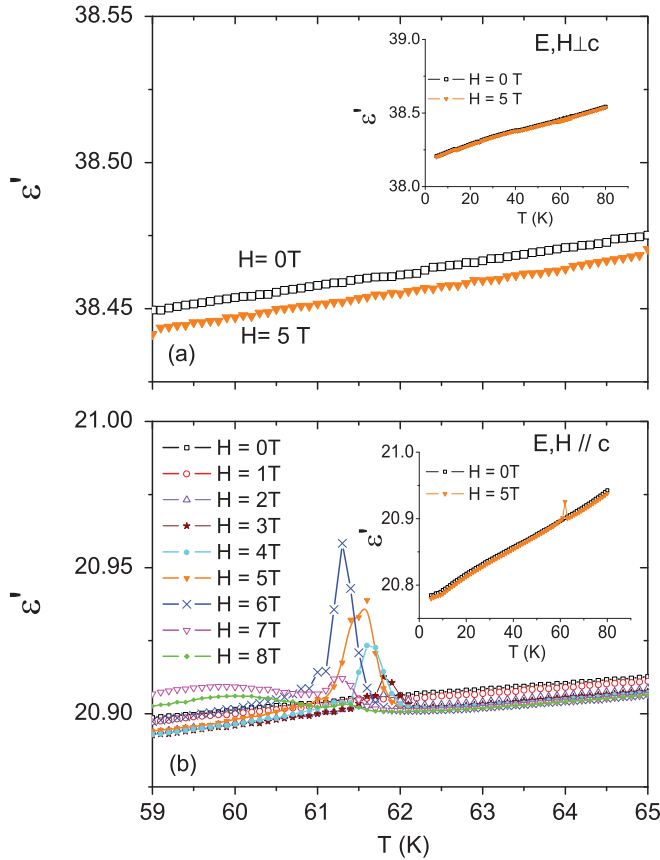
FIG. 3. (Color online) Temperature dependence of dielectric constant of MnTiO$_3$ (a) perpendicular to the c axis and (b) parallel to the c axis near T_N, measured in different applied fields. The inset shows the dielectric constant over an extended temperature range.

FIG. 4. (Color online) Temperature dependence of (a) pyroelectric current and (b) polarization of MnTiO$_3$ under magnetic field.

current and polarization for E, $H \parallel c$. At zero field, no anomaly in the pyroelectric current is observed. However, when a magnetic field is applied, an anomaly in the pyroelectric current corresponding to the onset of polarization is apparent; the broad peak increases in intensity with magnetic field up to 6 T and then decreases at 8 T, which is above the critical field for the spin-flop transition. The maximum polarization is 12 μC/m^2. We note that to measure the polarization it was necessary to cool the sample through T_N with simultaneously applied electric and magnetic fields to obtain a single AF domain. For E, $H \perp c$ we did not observe any polarization.

We also measured the polarization as a function of magnetic field, as shown in Fig. 5. The polarization is linear with respect to the applied field up to 3 T and becomes nonlinear at higher fields. This result confirms that MnTiO$_3$ is a linear magnetoelectric material.

IV. THEORETICAL APPROACH

Below we present a rather general theoretical analysis of the effect of magnetic fluctuations on the dielectric constant anomaly of magnetoelectric materials. Our phenomenological approach is based on symmetries of MnTiO$_3$ and is model independent. Earlier discussions of the effects of magnetoelectric coupling on the d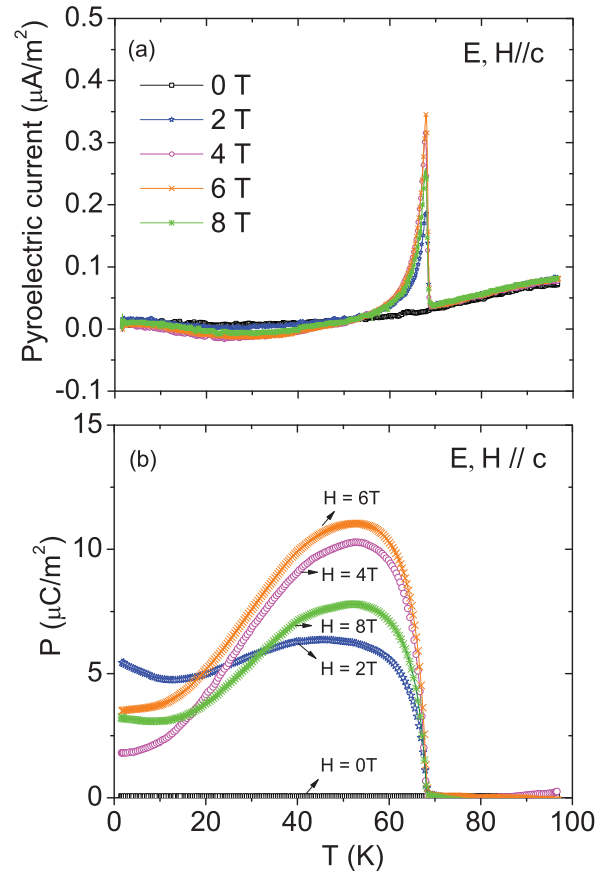ielectric properties pertained to the linear response in zero field, which is nonsingular.[30] We show that critical spin fluctuations near T_N lead to a divergent nonlinear magnetoelectric response, which explains the observed ε anomaly in the magnetic field.

The spin ordering in MnTiO$_3$ is described by the Néel order parameter $L = M_{1z} - M_{2z}$, where the indices 1 and 2 denote the positions of Mn ions in the unit cell, and z indicates that spins order parallel/antiparallel to the c axis.
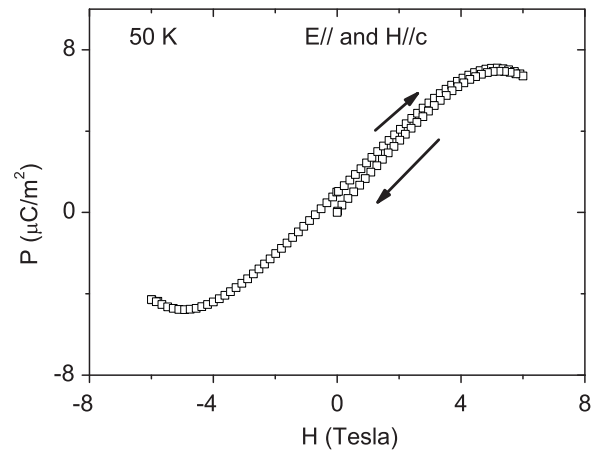

FIG. 5. Magnetic field dependence of polarization of MnTiO$_3$ at 50 K.

This ordering allows for three independent magnetoelectric couplings compatible with $R\bar{3}$ symmetry:

$$F_{\text{me}} = -g_{xx}L(E_xH_x + E_yH_y) - g_{xy}L(E_xH_y - E_yH_x) - g_{zz}LE_zH_z. \qquad (1)$$

In what follows we assume both electric and magnetic fields to be parallel to the c axis, $E = E_z$, $H = H_z$, and only consider the last term in Eq. (1), which gives rise to the magnetoelectric coefficient $\alpha_{zz} = g_{zz}\langle L\rangle$.

To model the behavior of the magnetic and dielectric susceptibilities in the vicinity of T_N, we consider the Landau free energy expansion

$$F(L,E,H) = F(L,0,0) - g_{zz}LEH + \frac{g_e}{2}L^2E^2 + \frac{g_m}{2}L^2H^2 - \frac{\chi_e^{(0)}E^2}{2} - \frac{\chi_m^{(0)}H^2}{2} + \cdots, \qquad (2)$$

where $F(L,0,0)$ is the free energy in the absence of external fields, g_e and g_m describe the coupling of the spin ordering to electric and magnetic fields, respectively, and $\chi_e^{(0)}(\chi_m^{(0)})$ is the "bare" dielectric (magnetic) susceptibility.

To describe the effect of spin fluctuations on the coupled magnetoelectric responses, we consider an effective free energy obtained by integrating over all possible realizations of the order parameter,

$$\mathcal{F}(E,H) = -k_BT \ln \int DL \exp\left[-\frac{1}{k_BT}\int dV\, F(L,E,H)\right]. \qquad (3)$$

The dielectric susceptibility is then given by

$$\chi_e = -\left.\frac{\partial^2\mathcal{F}}{\partial E^2}\right|_{E=0} = \chi_e^{(0)} - g_eL^2 + g_{zz}^2H^2k_BT\chi_L, \qquad (4)$$

where the second term describes the effect of spin ordering on the dielectric response in zero magnetic field, which for $MnTiO_3$ is very small, while

$$\chi_L = \frac{1}{k_BT}\int dV[\langle L(\mathbf{x})L(0)\rangle - \langle L\rangle^2] \qquad (5)$$

is the susceptibility to the staggered magnetic field equal to $+h(-h)$, for the Mn sublattice 1(2), which is linearly coupled to the primary order parameter of the transition L. This susceptibility diverges at the magnetic transition temperature: $\chi_L \propto |T - T_N|^{-\gamma}$, where the critical exponent $\gamma \sim 1.24$ for easy axis (Ising) magnets, while for isotropic Heisenberg magnets $\gamma \sim 1.39$ (Ref. 31). Since the last term in Eq. (4) is also proportional to H^2, it describes the magnetocapacitance that diverges at T_N.

The diagram in Fig. 6 illustrates how the effective coupling term proportional to E^2H^2, which gives rise to magnetocapacitance and is mediated by critical spin fluctuations, appears in the second order of expansion in the linear magnetoelectric coupling g_{zz}. Alternatively, in an applied magnetic field H, the magnetoelectric interaction $-g_{zz}LEH$ linearly couples the primary order parameter L to the electric field E, transforming the linear magnetoelectric material into a proper ferroelectric, which explains the divergence of the dielectric susceptibility.

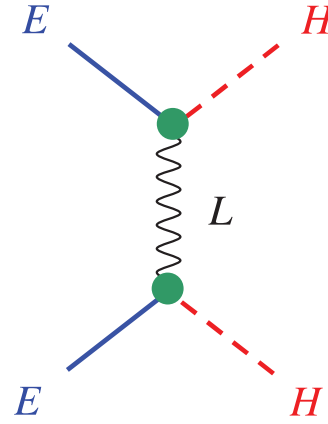Although the magnetocapacitance is proportional to the square of the weak magnetoelectric coupling g_{zz}, the

FIG. 6. (Color online) The effective coupling proportional to E^2H^2, which gives rise to magnetocapacitance, originating from the linear magnetoelectric coupling between L, E, and H.

divergence at T_N makes this effect easily observable. Critical spin fluctuations also give rise to the divergence of the magnetic susceptibility in an applied electric field, $\chi_m \propto g_{zz}^2E^2|T - T_N|^{-\gamma}$, and to nonlinear magnetoelectric effects (e.g., $P \propto g_{zz}g_mH^3|T - T_N|^{\beta-\gamma}$, where β is the critical exponent describing the temperature dependence of the order parameter L). These effects are, however, more difficult to observe.

V. DISCUSSION

Based on our polarization measurements (Figs. 4 and 5), it is clear that $MnTiO_3$ displays linear magnetoelectric coupling, with the magnetoelectric coefficient $\alpha_{zz} \sim 5 \cdot 10^{-5}$ in Gaussian units. The polarization appears when a magnetic field is applied along the hexagonal c axis and exhibits a linear response to the field when measured at constant temperature.

Furthermore, we have found that in $MnTiO_3$ there is no dielectric anomaly at T_N in zero field. Some magnetic materials [e.g. hexagonal $YbMnO_3$ (Refs. 32,33)] show a rather strong ε anomaly, resulting from the spin-lattice coupling and described by the $\frac{g_e}{2}L^2E^2$ term in the free energy Eq. (2). We thus conclude that the spin-lattice coupling in $MnTiO_3$ is weak. Nevertheless, the dielectric constant shows a clearly discernible peak at T_N when a magnetic field is applied along the hexagonal c axis [Fig. 3(b)], the intensity of which increases with increasing magnetic field up to 6 T. The appearance of this dielectric anomaly coincides with the emergence of induced polarization (Fig. 4).

To confirm the theory outlined in Sec. IV, we have scaled the dielectric constant in the vicinity of $T_N(H)$ by first subtracting the extrapolated linear background fitted above $T_N(H)$ to give $\varepsilon^* = \varepsilon - (a + bT)$, then dividing ε^* by H^2. A plot of ε^*/H^2 versus $T - T_N(H)$ for different measurement fields is shown in Fig. 7, confirming that ε is indeed proportional to H^2 at $T_N(H)$ in fields of $0 \leqslant H \leqslant 6$ T. For $H \geqslant 7$ T the dielectric constant no longer scales with H^2, which can be ascribed to the previously reported spin flop transition.[24] The inset to Fig. 7 shows a fit to the divergence of ε measured in 5 T in the region immediately above T_N, where $\varepsilon \propto |T - T_N|^{-\gamma}$. As predicted
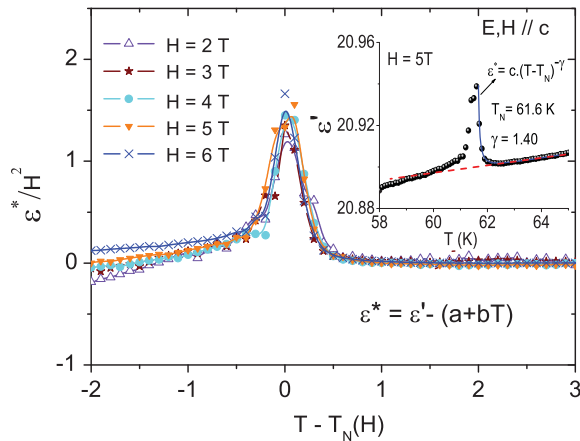
FIG. 7. (Color online) Dielectric constant scaled by H^2 plotted as a function of $T - T_N(H)$ for E, H parallel to the c axis. The inset shows a fit to the divergence of the dielectric constant immediately above T_N, demonstrating critical behavior.

in Sec. IV, behavior indicative of critical spin fluctuations is clearly observed. However, the critical exponent γ above T_N is strongly dependent on the choice of background and $T_N(H)$ used in the fitting process; the value extracted at different fields lies in the range 1.2 to 1.8 and thus we are unable to make an unambiguous distinction between Ising and Heisenberg magnets.[31] We note that Akimitsu *et al*. obtained a critical exponent of 1.22 from neutron scattering measurements, close to that expected for a three-dimensional Ising magnet.[34,35]

The good agreement between our experimental findings and theoretical analysis demonstrates that MnTiO₃ exhibits linear magnetoelectric coupling, which generates nonlinear magnetoelectric responses mediated by critical spin fluctuations and gives rise to the magnetocapacitance that diverges at T_N. As mentioned above, this result can easily be understood by noting that in nonzero magnetic fields, the LEH (or LMP) coupling present in linear magnetoelectrics couples the polarization P directly to the primary antiferromagnetic order parameter L. This gives rise to a divergence in the dielectric susceptibility at T_N, similar to that of a proper ferroelectric near the critical temperature. The coupling between P and L is proportional to H, implying that the magnitude of the anomaly scales with H^2, in agreement with experimental observations. We note that the dielectric constant anomaly induced by an applied magnetic field in MnTiO₃ does not originate from magnetostriction,

which is rather weak in this material, as one can conclude from the absence of any ε anomaly in zero field. In fact, the weak magnetostriction might be crucial for the observation of the field-induced singularity: strong spin-lattice coupling transforms the second-order phase transition into a first-order one, thereby suppressing fluctuations of the magnetic order parameter, which give rise to the dielectric constant anomaly. We also note that the linear coupling between P and L present in an applied magnetic field makes it possible to move antiferromagnetic domain walls with an applied electric field. The temperature dependence of the dielectric anomaly may thus be governed by the dynamics of pinned antiferromagnetic domain walls, as is the case for multiferroic DyMnO₃ showing the giant magnetocapacitance effect.[16]

VI. CONCLUSION

We have shown that MnTiO₃ is a linear magnetoelectric material. We demonstrate that there is no dielectric anomaly at the onset of magnetic ordering in the absence of an applied magnetic field. However, a sharp dielectric peak does appear at T_N when a magnetic field is applied. This phenomenon is associated with the free energy term LMP, where in finite magnetic fields the polarization P couples directly to the antiferromagnetic order parameter L. By modeling the magnetic and dielectric properties based on a Landau free energy expansion, we have shown that the dielectric constant close to T_N is proportional to the square of the magnetic field, which we have confirmed experimentally. This provides an easy method to recognize antiferromagnetic linear magnetoelectric materials, circumventing the experimental difficulties that are often involved in measuring polarization.

*nandangmufti@gmail.com

[1] D. Khomskii, Physics **2**, 20 (2009).

[2] T. Kimura, S. Ishihara, H. Shintani, T. Arima, K. T. Takahashi, K. Ishizaka, and Y. Tokura, Phys. Rev. B **68**, 060403(R) (2003).

[3] G. Lawes, A. B. Harris, T. Kimura, N. Rogado, R. J. Cava, A. Aharony, O. Entin-Wohlman, T. Yildrim, M. Kenzelmann, C. Broholm, and A. P. Ramirez, Phys. Rev. Lett. **95**, 087205 (2005).

[4] H. Katsura, N. Nagaosa, and A. V. Balatsky, Phys. Rev. Lett. **95**, 057205 (2005).

[5] M. Mostovoy, Phys. Rev. Lett. **96**, 067601 (2006).

[6] L. C. Chapon, P. G. Radaelli, G. R. Blake, S. Park, and S.-W. Cheong, Phys. Rev. Lett. **96**, 097601 (2006).

[7] T. Arima, J. Phys. Soc. Jpn. **76**, 073702 (2007).

[8] S.-W. Cheong and M. Mostovoy, Nature Mater. **6**, 13 (2007).

[9] Y. J. Choi, H. T. Yi, S. Lee, Q. Huang, V. Kiryukhin, and S.-W. Cheong, Phys. Rev. Lett. **100**, 047601 (2008).

[10] T. Kimura, T. Goto, H. Shintani, K. Ishizaka, T. Arima, and Y. Tokura, Nature (London) **426**, 55 (2003).

[11] N. Hur, S. Park, P. A. Sharma, J. S. Ahn, S. Guha, and S.-W. Cheong, Nature (London) **429**, 392 (2004).

[12] Y. Yamasaki, S. Miyasaka, Y. Kaneko, J.-P. He, T. Arima, and Y. Tokura, Phys. Rev. Lett. **96**, 207204 (2006).

[13] Y. J. Choi, J. Okamoto, D. J. Huang, K. S. Chao, H. J. Lin, C. T. Chen, M. van Veenendaal, T. A. Kaplan, and S.-W. Cheong, Phys. Rev. Lett. **102**, 067601 (2009).

[14] K. Kimura, H. Nakamura, S. Kimura, M. Hagiwara, and T. Kimura, Phys. Rev. Lett. **103**, 107201 (2009).

[15] T. Goto, T. Kimura, G. Lawes, A. P. Ramirez, and Y. Tokura, Phys. Rev. Lett. **92**, 257201 (2004).

[16] F. Kagawa, M. Mochizuki, Y. Onose, H. Murakawa, Y. Kaneko, N. Furukawa, and Y. Tokura, Phys. Rev. Lett. **102**, 057604 (2009).

[17] N. Hur, S. Park, P. A. Sharma, S. Guha, and S.-W. Cheong, Phys. Rev. Lett. **93**, 107207 (2004).

[18] L. D. Landau and E. M. Lifshitz, *Electrodynamics of Continuous Media* (Pergamon, Oxford, 1984).

[19] A. S. Borovik-Romanov and H. Grimmer, in *Magnetic Properties*, International Tables for Crystallography Vol. D, edited by A. Authier (Kluwer, Dordrecht, 2003), pp. 105–149.

[20] M. Fiebig, J. Appl. Phys. D **38**, R123 (2005).

[21] G. Shirane, S. J. Pickart, and Y. Ishikawa, J. Phys. Soc. Jpn. **14**, 1352 (1959).

[22] J. J. Stickler, S. Kern, A. Wold, and G. S. Heller, Phys. Rev. **164**, 765 (1967).

[23] J. Akimitsu, Y. Ishikawa, and Y. Endoh, Solid State Commun. **8**, 87 (1970).

[24] H. Yamauchi, H. Hiroyoshi, M. Yamada, H. Watanabe, and H. Takei, J. Magn. Magn. Mater. **31-34**, 1071 (1983).

[25] G. A. Samara and P. T. Richards, Phys. Rev. B **14**, 5073 (1976).

[26] A. K. Zvezdin, G. P. Vorob'ev, A. M. Kadomtseva, Yu. F. Popov, D. V. Belov, and A. P. Pyatakov, J. Exp. Theor. Phys. **109**, 221 (2009).

[27] M. S. Seehra and R. E. Helmick, Phys. Rev. B **24**, 5098 (1981).

[28] M. S. Seehra and R. E. Helmick, J. Appl. Phys. **55**, 2330 (1984).

[29] J. Ko and C. T. Prewitt, Phys. Chem. Miner. **15**, 355 (1988).

[30] G. T. Rado, Phys. Rev. **128**, 2546 (1962).

[31] P. M. Chaikin and T. C. Lubensky, *Principles of Condensed Matter Physics* (Cambridge University Press, Cambridge, England, 1995).

[32] U. Adem, M. Mostovoy, N. Bellido, A. A. Nugroho, C. Simon, and T. T. M. Palstra, J. Phys. Condens. Matter **21**, 496002 (2009).

[33] A. A. Nugroho, N. Bellido, U. Adem, G. Nènert, C. Simon, M. O. Tjia, M. Mostovoy, and T. T. M. Palstra, Phys. Rev. B **75**, 174435 (2007).

[34] J. Akimitsu and Y. Ishikawa, Solid State Commun. **15**, 1123 (1974).

[35] J. Akimitsu and Y. Ishikawa, J. Phys. Soc. Jpn. **42**, 462 (1977).